

Depth Estimation of Thermal Image with Lightweights Model

Anonymous CVPR submission

Paper ID ****

Abstract

This paper focuses on lightweight modifications to the published thermal image depth estimation model, SupDepth4Thermal[17], and evaluates their effects on efficiency and accuracy. All models are trained validated and tested with the Multi-Spectral Stereo (MS^2) thermal image dataset, with training parameters referenced from the original paper[17]. First, the performance of the Lite-Mono[23] model in monocular depth estimation (MDE) is examined. The results show that Lite-Mono significantly reduces the mean inference time by 75% , from 40.58 ms to 10.28 ms, while the AbsRel error increases from 0.125 to 0.527. Next, in stereo depth estimation (SDE), the original Neural Window Conditional Random Field (NeWCRF) decoder in SupDepth4Thermal is replaced with depthwise separable convolutions. This leads to a substantial reduction in the inference time and Flops. However, the error rate deteriorated sharply. Finally, a new model is proposed by integrating the Lite-Mono core encoder, Parameterized Cost Volume (PCV) [22] construction, and the NeWCRF decoder. This configuration reduces the number of trainable parameters to roughly one-tenth of the original, lowers mean inference time by about 6%, and keeps the overall accuracy reasonably close to the original model, with moderate degradations (e.g., D1-all increases by about 6% on average). My source code is available at my GitHub.

1. Introduction

Depth estimation using thermal images has great potential because Long-Wave Infrared (LWIR) signals remain reliable in undesirable conditions such as low light and rain [12]. However, prior lightweight models and advanced depth estimation algorithms are mostly evaluated on RGB[20, 23], while systematic, reproducible studies on thermal remain scarce. Moreover, thermal images are single-channel and often texture-poor, making the task more challenging. In this paper, I propose three modifications to the existing thermal depth estimation model, SupDepth4Thermal[17], and investigate their efficiency and

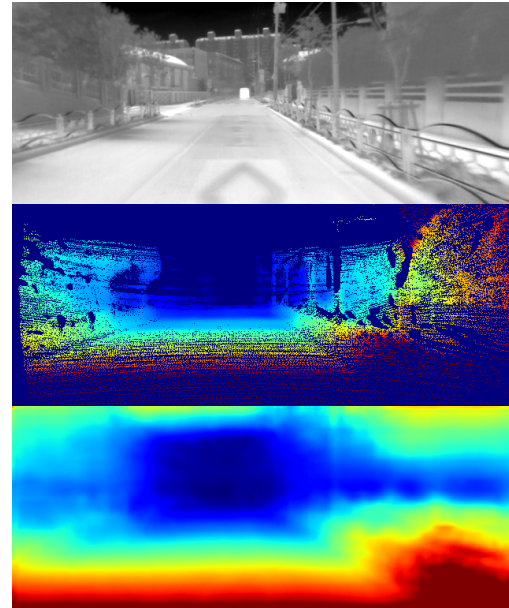


Figure 1. Testing result of the model integrated with the Lite-Mono encoder and PCV The original thermal image is from MS^2 daytime testset. From top to bottom: Thermal image, Ground Truth(GT) disparity map and stereo disparity estimation

performance.

I choose to make the model lightweight due to limited computing resources. I can only run my algorithms and store all data on RCAC Scholar, where storage space is limited and GPU access is not always available (4-hour allocations with uncertain queue times). Therefore, a lightweight model is more suitable to reduce memory consumption and computing time.

In this paper, SupDepth4Thermal serves as the foundation for all implementations. The three modifications focus on these ideas:

- How does a Lite-Mono-style light encoder perform for thermal MDE?
- Can depthwise separable convolutions network replace SupDepth4Thermal's heavy decoder, NeWCRF blocks, in thermal SDE?

- 054 • Will integrating a Lite-Mono encoder together with
055 a PCV computation method yield a better accuracy–efficiency trade-off in thermal SDE?
056

057 In all three experiments, the MS^2 dataset is used for
058 training, validation, and testing. The dataset splits follow
059 the settings of Shin *et al.*, and all other training hyperpara-
060 meters are kept the same as in their work. The scripts for
061 training, testing, timing, and FLOPs evaluation are also the
062 original implementations of Shin *et al.* The results of the
063 three modifications are as follows:

- 064 • Lite-Mono for MDE: greatly shortens mean inference
065 time to 25%, but accuracy drops at the same time. The av-
066 erage AbsRel increases from 0.125 to 0.527, SqRel from
067 1.130 to 6.739, and RMSE from 5.191 to 13.134.
068 • Depthwise separable decoder for SDE: replaces most of
069 NeWCRF’s heavy computation. The mean inference time
070 remains only 59% of the original. However, this comes at
071 the cost of a noticeable degradation in accuracy:: EPE-all
072 increases 26%, D1-all increases 44%.
073 • Lite-Mono encoder plus PCV strategy for SDE: reduces
074 parameters markedly by 10 times, while accuracy de-
075 grades: EPE-all increases 15%, D1-all increases 6.6%.

076 2. Related Work

077 2.1. MS^2 Dataset

078 MS^2 is a large outdoor dataset that includes about 195k
079 pairs of synchronized and rectified multi-spectral stereo
080 sensor data. It is multi-spectral, comprising RGB, near-
081 infrared (NIR), long-wave infrared (LWIR), LiDAR, GNSS,
082 and IMU. Those sufficient stereo data pairs support the
083 construction of both MDE and SDE models. This was not pos-
084 sible for other benchmark datasets at the time because they
085 were either indoor or had limited depth of field, making
086 them less suitable for long-distance depth applications.

087 In addition, the dataset spans day, night, and rain con-
088 ditions and also includes different scenes such as campus,
089 residential, road, and suburban, providing robustness stud-
090 ies and realistic deployment evaluation.

091 MS^2 has been actively used in recent research. For ex-
092 ample, Raviglia *et al.* leverages MS^2 to study RGB to IR
093 data augmentation, synthesizing realistic infrared appear-
094 ances from RGB images[15]. Zou *et al.* develop Mono-
095 TherDepth, a monocular thermal depth model trained and
096 evaluated on MS^2 [25]. These works illustrate MS^2 ’s utility
097 for both cross-spectral learning and thermal-specific depth
098 estimation benchmarks.

099 2.2. SupDepth4Thermal

100 SupDepth4Thermal is a single model that can run both
101 MDE and SDE on thermal (LWIR) images. Its backbone,
102 Swin transformer, extracts a four-level feature pyramid (at

1/4, 1/8, 1/16, 1/32 of the input size). A pyramid pool-
103 ing head injects global context, and the decoder consumes a
104 3D correlation cost volume when a right image is available.
105 When only a left image is provided, which is under MDE
106 operation, the same decoder operates with a zero-filled cost
107 volume, so one architecture naturally “bridges” the mono
108 and stereo tasks.

109 To be more specific, the functions of each module are as
110 follows:

- 111 • Swin Transformer[11]: This transformer uses windowed
112 self-attention plus shifted windows to link information
113 across neighboring windows, yielding a hierarchical rep-
114 resentation with good locality, efficiency, and long-range
115 modeling. It is a generous vision backbone that can work
116 on image classification, object detection and semantic
117 segementation[1].
- 118 • PPM[24]: PPM performs multi-scale global pooling on
119 the highest-level feature map and mixes those pooled de-
120 scriptors back into the stream. This supplies scene-level
121 context (layout, object extent) that complements weak lo-
122 cal textures and stabilizes the decoder’s predictions.
- 123 • Cost-Volume Construction: Shin *et al.* apply correlation
124 cost volume at each scale. For each disparity d , it mea-
125 sures the inner-product similarity between the left feature
126 at (x, y) and the right reference at $(x - d, y)$ as the cost
127 volume C :

$$C^{scale}(d, x, y) = (1/N_c) * \langle f_L(x, y), f_R(x - d, y) \rangle \quad 129$$

- 130 • NewCRF[21]: NewCRF fuses multi-scale features and the
131 cost volume cues under a CRF-like regularization learned
132 by a neural network. The neural window operations ag-
133 gregate evidence within local windows, and the connected
134 CRF encourages pixels with similar appearance to have
135 compatible depths, while preserving sharp boundaries

136 Shin *et al.* evaluate the error rate and accuracy of
137 SupDepth4Thermal with other MDE and SDE networks.
138 The results show that it has competitive performance.

139 2.3. Lite-Mono

140 Lite-Mono is a lightweight model originally designed for
141 RGB MDE that aims to keep accuracy competitive while
142 cutting parameters, FLOPs, and latency. Zhang *et al.* put
143 most effort on the design of the encoder which contains two
144 major parts, Continuous Dilated Convolution (CDC) block
145 and Local-Global Feature Interaction (LGFI) block. CDC
146 block expands the effective receptive field via dilated depth-
147 wise 3×3 filters (for local structure) while keeping computa-
148 tion low, and LGFI block adds lightweight channel-wise at-
149 tention to propagate scene-level cues that stabilize ambigu-
150 ous regions.

151 In spite of the small model size of Lite-Mono, it still
152 has good edge fidelity. Dynamo-Depth [18]is interested

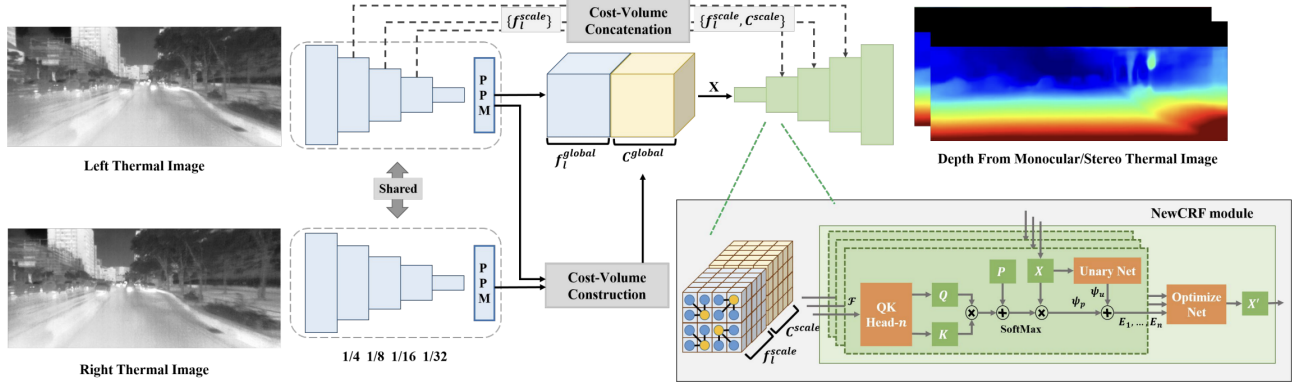


Figure 2. **Pipeline of SupDepth4Thermal** This network can do both MDE and SDE from given single or stereo thermal image. The network combined with three major parts, encoder, cost volume and decoder. In the beginning, Swin-Transformer downsamples the image and extracts the feature maps and Pyramid Pooling Module(PPM) aggregates the global context. Next, the 3D cost-volume is computed. If there is right thermal image, its cost volume will be combined into left one; otherwise, if only left image available, the network will view the right volume as zero-filled. Afterward, the volume and feature maps will be send into NewCRF based decoder, and carry out the final depth estimation

Table 1. **Comparison between MS² and other benchmark datasets.** Before the later published FIReStereo dataset, MS² addressed the lack of large-scale outdoor infrared imagery.

Dataset	Year	Environment	Platform	Total # of Data Pairs
MS ² [17]	2022	Outdoor	Vehicle	195k
CATS [19]	2017	In\Outdoor	Handheld	1.4k
KAIST [2]	2018	Outdoor	Vehicle	Unknown
MultiSpectralMotion [4]	2021	In\Outdoor	Handheld	121k\27.3k
ViViD++ [8]	2022	Outdoor	Vehicle	5.6k
OdomBeyondVision [9]	2022	Indoor	Handheld\UGV\UAV	71k\117k\21k
FIReStereo [5]	2025	Outdoor	UAV	102k

in Lite-Mono precisely for this accuracy–efficiency balance: a compact encoder leaves compute headroom for temporal modules (e.g., motion-aware warping, recurrent refinement), while CDC delivers sharp per-frame edges and LGFI contributes global semantics that make temporal fusion more stable. In practice, Dynamo-Depth uses Lite-Mono as the backbone encoder, then stacks a temporal head on top to aggregate features across adjacent frames, improving dynamic-scene depth without significantly increasing latency or parameters.

Zhang *et al.* evaluate different size of Lite-Mono networks with other representative networks on KITTI[6] dataset. The results indicate that Lite-Monos not only have higher accuracy and lower error, but also have relatively small size.

2.4. Depthwise Separable Convolutions

The popularity of depthwise separable convolution can be attributed to its integration into models like Xception[3]

and MobileNet[7]. Depthwise convolution performs spatial filtering independently on each input channel. Instead of applying a single convolutional kernel across all channels, it assigns a separate spatial kernel to each channel, efficiently enlarging the receptive field and capturing local structures. This design greatly reduces the number of parameters and computational cost compared to standard convolutions, while preserving strong representational power.

The reason I use depthwise separable convolution is because I want to replace the NewCRF module with a Lite-Mono-style decoder. The similarity between Lite-Mono and depthwise separable convolution is that both follow a “local spatial filtering + channel mixing” design. They all emphasize the cheapest way to build effective receptive fields and feature representations.

One of the classic applications that implements depthwise separable convolution is FastDepth[20]. FastDepth adopts a lightweight architecture where depthwise separable convolutions are used extensively. The application of

153

154

155

156

157

158

159

160

161

162

163

164

165

166

167

168

169

170

171

172

173

174

175

176

177

178

179

180

181

182

183

184

185

186

187

188

189

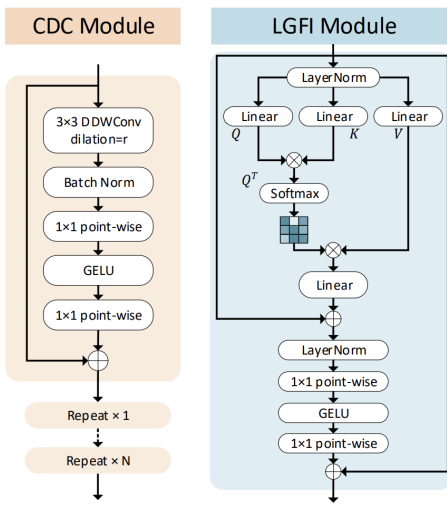


Figure 3. **Pipeline of CDC block and LGFI block.** CDC module utilizes dilated convolutions to extract multi-scale local features. LGFI module take advantage of the self-attention mechanism to encode long range global information into the features.

this network reduce the FLOPs and parameters while maintaining reasonable accuracy. This design enables real-time monocular depth estimation on embedded or mobile devices, with a very small model size and fast inference speed compared to conventional CNN-based depth networks.

2.5. PCV

Traditional stereo builds a 3D/4D cost volume ($H \times W \times D \times C$) which requires large number of memory and computation. Although iterative method like recurrent update[10] could reduce memory usage, it still takes several iterations to converge which cost time. Instead of representing each pixel's disparity evidence with a dense D -slice volume, PCV method represents its disparity distribution using only K Gaussians components. That is, each pixel then keeps just a few parameters, effectively compressing the entire disparity curve. The concept of PCV is like:

$$p(d | x, y) = \sum_{i=1}^K \alpha_i(x, y) \mathcal{N}(d; \mu_i(x, y), \sigma_i^2(x, y))$$

α_i is weight, μ_i is mean and σ_i is variance. It reveals that PCV reduces the cost volume parameters from traditional ($H \times W \times D \times C$) to ($H \times W \times 3K$). In Zeng *et al.* experiments, PCV indeed achieves the intended effect. On the SceneFlow[13], KITTI[6], Middlebury[16], and Booster[14] datasets, it reduced the runtime by about 4 to 15 times compared with RAFT-Stereo[10], without sacrificing accuracy.

3. Method

3.1. Set Up

All experiments are conducted by using RCAC Scholar serve. I download the source code of SupDepth4Thermal, Lite-Mono and PCV from the following GitHub repositories:

- SupDepth4Thermal: <https://github.com/UkcheolShin/SupDepth4Thermal>
- Lite-Mono: <https://github.com/noahzn/Lite-Mono>
- PCV: <https://github.com/jiaxiZeng/Parameterized-Cost-Volume-for-Stereo-Matching>

For the MS² dataset, it is required to visit the official website <https://sites.google.com/view/multi-spectral-stereo-dataset> and fill a survey form. Afterward, I receive an email with the instructions and download links.

I only download the "sync_data" and the "proj_depth" folders because this paper only requires those data. I store them under RCAC Scholar personal "/scratch" directory, considering their over 200G storage requirement, and also delete the source zipped files right after the unaip in order to remain sufficient space.

The Conda environment setting could be referenced to "environment.yaml" in my GitHub repository. All experiments are developed and tested in the following package:

- OS: Rocky Linux 9.6 (Blue Onyx)
- CUDA: 12.1.105
- PyTorch: 2.3.0+cu121
- Python: 3.10.19

To mitigate unexpected interruption on RCAC Scholar, I adopt the checkpoints mechanism in training script. Checkpoints are saved when any of the following three conditions is met: every 500 steps, at the end of each epoch and upon achieving a new lowest validation loss.

3.2. Optimizer and Data Augmentation

All models are trained on RCAC Scholar using NVIDIA V100 (16 GB), A40 (48 GB), or A30 (24 GB) GPUs. MDE model is trained for 30 epochs; SDE models for 60 epochs. All other training hyperparameters and setting are aligned with those of Shin *et al.*

3.3. Source Code Modification

In general, I create dedicated yaml files and trainer scripts for each modification experiment. Moreover, I edit every "__init__.py" file to ensure the targeted files could be imported correctly.

- Lite-Mono for MDE: In the codebase, this model is registered as "litemono". From the source repository, I reuse only "depth_encoder", "depth_decoder", and "layers". I

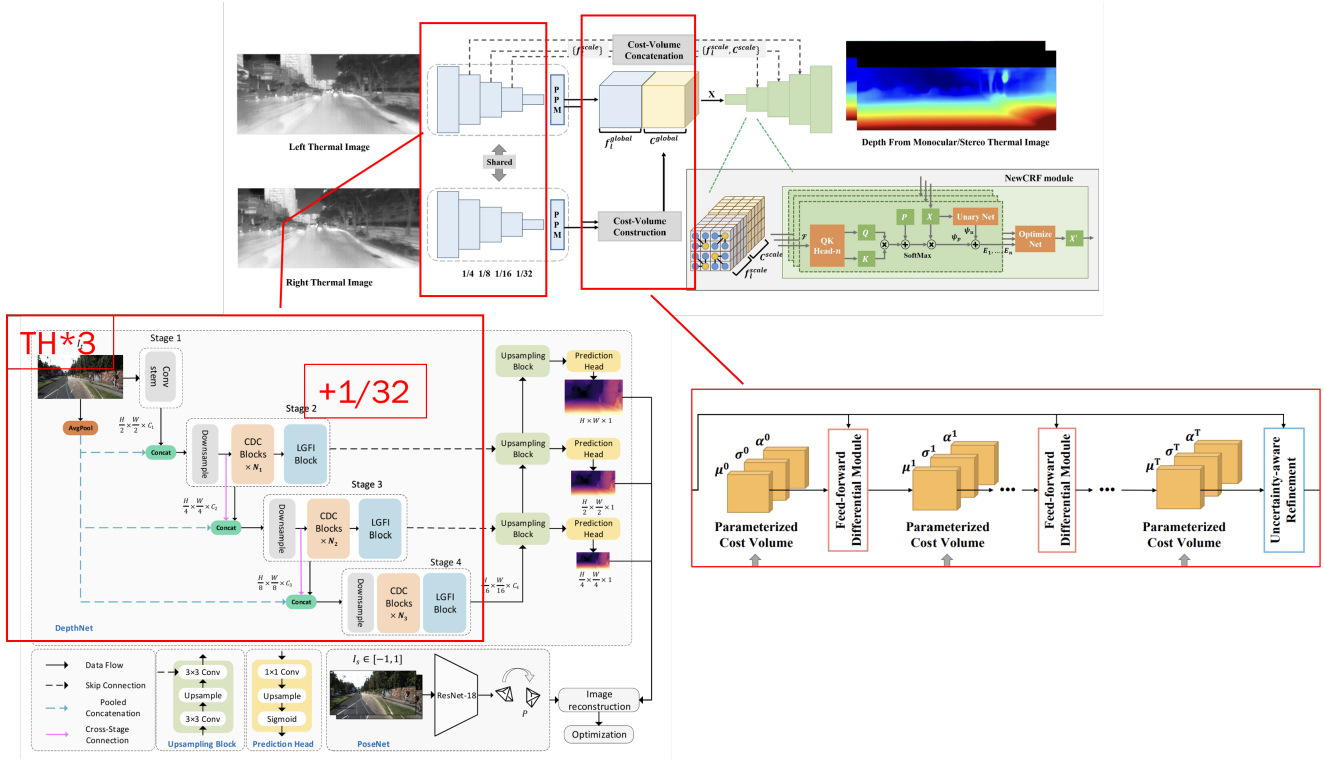


Figure 4. Pipeline of Lite-Mono encoder plus PCV strategy for SDE The original swin transformer is replaced with Lite-Mono encoder, and the correlation cost volume method also be replaced with PCV. Since Lite-Mono take 3-channels input, thermal image data is replicated into 3 times. An additional 1/32 scale is prepared for the NewCRF module.

265 exclude "resnet_encoder", as Lite-Mono does not rely on
266 a ResNet backbone. The "pose_decoder" is also omitted:
267 the base model uses GT-depth supervision, so no self-
268 supervised photometric pose is needed.
269

270 Since Lite-Mono expects RGB, the 1-channel thermal
271 input is channel-replicated ($\times 3$) to conform to the 3-
272 channel interface.

- 273 • Depthwise separable decoder for SDE: In the codebase,
274 this model is registered as "LiteMono_crf", although it
275 primarily retains only the Lite-Mono-style depthwise
276 convolution design. The overall framework of this net-
277 work is adapted from "ms_crf" directory which created
278 by Shin *et al.* I duplicate the directory and refactore its
279 contents. The primary distinction is dedicated head, "lite-
280 mono_head", which plugs in a depthwise design. Further-
281 more, I drop the original NewCRF decoder pattern
282 Another crucial alteration is in the "multiscale_loss" func-
283 tion of its trainer,"LiteMono_crf". I revise the disparity to
284 depend on itself, the weight GT and weight prediction.
- 285 • Lite-Mono encoder plus PCV strategy for SDE: In the
286 codebase, this model is registered as "LiteMonoEn".
287 I reuse not only "depth_encoder", "depth_decoder",
288 and "layers" from Lite-Mono repository, but also
289 "corr", "update" and "utils" from pcv/core repository.

290 This model is also derived from "ms_crf". I specifically
291 create a file "LiteMonoEn" to bridge the Lite-Mono en-
292 coder, PCV, and the original NeWCRF module. In addi-
293 tion, I prepare a new file "pcv_module" for pcv to inter-
294 face the features after PPM.

295 A major modification in this model is to align the origi-
296 nal three-scale LiteMono architecture with the four-scale
297 NeWCRF. Therefore, I add an extra 1/32 scale inside
298 Lite-Mono encoder. Beyond that, considering PCV de-
299 fault 1/4 input scale, it extracts features at 1/4 and then
299 feeds the output into NeWCRF initial 1/32 stage.

4. Result

4.1. Lite-Mono for MDE:

300 From Tab. 2, compared with original SupDepth4Thermal,
301 Lite-Mono network variant reduces the parameter count by
302 roughly 88 times, decreases FLOPs by about 24 times, and
303 achieves nearly 4 times faster inference.

304 However, from Tab. 3, SupDepth4Thermal achieves an
305 average AbsRel of about 0.125 and $\delta < 1.25$ of about 0.88.
306 In contrast, Lite-Mono yields an average AbsRel of about
307 0.527—roughly four times larger—and $\delta < 1.25$ of only
308 around 0.30, indicating a significant degradation in depth
309

289

290

291

292

293

294

295

296

297

298

299

299

300

301

302

303

304

305

306

307

308

309

310

Table 2. **Comparison between SupDepth4Thermal Mono network and Lite-Mono network.** “#Parameters” counts trainable weights; “#FLOPs” denotes floating-point operations per forward pass; “Mean inference time” is averaged over the evaluation set. Lower is better.

Model	#Parameter of Shape	#Flops	Mean inference time
SupDepth	0.27G	0.158T	40.580
Lite-Mono	3.075M	6.713G	10.282

311 accuracy.

312 In summary, the LiteMono-based model is highly effi-
 313 cient in terms of model size, computation, and runtime, but
 314 in the current configuration this efficiency is obtained at the
 315 cost of a substantial loss in depth accuracy.

316 4.2. Depthwise separable decoder for SDE:

317 The major difference between the original SDE model and
 318 depthwise separable network lies in the replacement of the
 319 NeWCRF decoder.. The results from Tab. 5 indicate that
 320 NewCRF is a heavy module, with immense parameters and
 321 substantial computing time. However, from Tab. 4, it reveals
 322 that the new depthwise separable convolution model fails to
 323 maintain accuracy. In other words, the gain in speed comes
 324 at the cost of degraded performance in this modification.

325 4.3. Lite-Mono encoder plus PCV strategy for SDE:

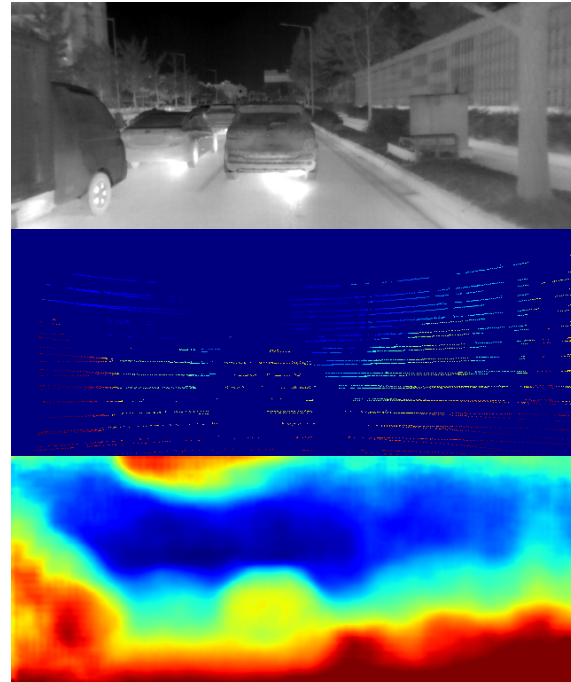
326 In contrast to the previous modification, in this section, the
 327 encoder and cost-volume computation algorithm is replaced
 328 from original SDE model. The Tab. 5 results show that this
 329 new model does become lightweight. However, the infer-
 330 ence time just slightly improve. Although the combination
 331 of Lite-Mono encoder and PCV make the model lighter, the
 332 error rate of new model still increase: EPE-all increases
 333 15%, D1-all increases 6.6%.

334 4.4. Comparison between new SDE models

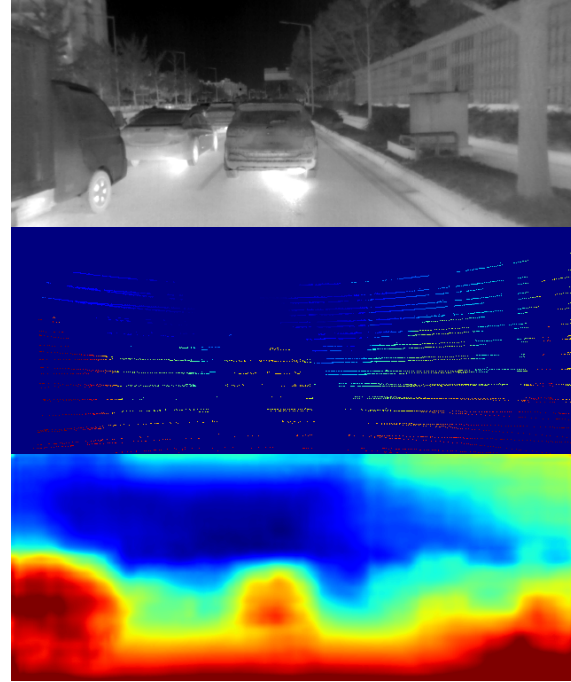
335 According to Tab. 4, the Lite + PCV model has better accu-
 336 racy than Depthwise model. This outcome could be exam-
 337 ined in Fig. 5. The prediction from depthwise model is not
 338 only inaccurate for the car in the center, whose estimated
 339 depth does not approach the orange GT region, but also un-
 340 stable in the surrounding areas. The truck on the left is not
 341 highlighted with a consistent red region, spurious red noise
 342 appears in the sky at the top, and the electrical box on the
 343 right side in the grass is not detected at all.

344 4.5. Discussion

345 There are still many potential modifications to explore. For
 346 example, one could fully replace SupDepth4Thermal by



(a) Test result from Depthwise model.



(b) Test result from Lite + PCV model.

Figure 5. **Comparison between new SDE models** Both figures are generated from the rain scenario of the testing dataset and correspond to sample 01930. In each sub-figure, from top to bottom: Thermal image, GT disparity map and stereo disparity estimation

347 combining LiteMono, PCV, and depthwise separable con-
 348 volutions into a single unified architecture.

Table 3. **Comparison of MDE models performance.** AbsRel, SqRel, RMSE, RMSElog (lower is better) and accuracy thresholds $\delta < 1.25, \delta < 1.25^2, \delta < 1.25^3$ (higher is better).

Model	Test set	Error				Accuracy		
		AbsRel	SqRel	RMSE	RMSElog	$\delta < 1.25$	$\delta < 1.25^2$	$\delta < 1.25^3$
SupDepth4Thermal (Mono)	Day	0.115	0.983	4.895	0.201	0.882	0.952	0.977
	Night	0.107	0.850	4.658	0.185	0.894	0.961	0.981
	Rain	0.152	1.567	6.020	0.247	0.822	0.928	0.964
	Avg	0.125	1.130	5.191	0.211	0.866	0.947	0.974
LiteMono (DepthNet encoder)	Day	0.539	6.794	13.571	0.644	0.286	0.519	0.696
	Night	0.486	5.611	12.377	0.592	0.306	0.556	0.740
	Rain	0.558	7.811	13.455	0.638	0.308	0.535	0.708
	Avg	0.527	6.739	13.134	0.625	0.900	0.537	0.715

Table 4. **SDE performance comparison.** EPE-all, D1-all, and bad-pixel ratios $>1\text{px}$, $>2\text{px}$, $>3\text{px}$ are reported on the day, night, and rain test sets (lower is better)

Lower is better						
Model	Test set	EPE-all (px)	D1-all (%)	$>1\text{px}$ (%)	$>2\text{px}$ (%)	$>3\text{px}$ (%)
SupDepth4Thermal	Day	0.957	5.7	22.7	9.1	5.7
	Night	0.853	4.8	21.3	8.2	4.8
	Rain	1.159	7.7	29.1	12.4	7.7
	Avg	0.990	6.1	24.4	9.9	6.1
Depwise	Day	1.040	6.0	33.1	12.9	6.0
	Night	1.310	9.7	41.3	18.6	9.7
	Rain	1.404	10.7	46.9	21.4	10.8
	Avg	1.251	8.8	40.4	17.6	8.8
Lite + PCV	Day	1.021	5.3	34.1	12.1	5.3
	Night	1.105	5.5	40.4	13.9	5.5
	Rain	1.293	8.8	44.5	18.3	8.8
	Avg	1.140	6.5	39.7	14.8	6.5

Table 5. **Comparison between SupDepth4Thermal SDE network, Depwise separable decoder network (Depwise) and Lite-Mono plus PCV network (Lite+PCV).** “#Parameters” counts trainable weights; “#FLOPs” denotes floating-point operations per forward pass; “Mean inference time” is averaged over the evaluation set. Lower is better.

Model	#Parameter of Shape	#Flops	Mean inference time
SupDepth	0.284G	0.322T	96.537
Depwise	61.46M	47.457G	56.929
Lite+PCV	19.381M	80.764G	90.540

349 In addition, there is still a large hyperparameter space to
350 investigate. For LiteMono, I currently use the tiny configura-
351 tion, but the small, normal, and 8M variants size could

also be tested. Training hyperparameters such as learning rate, batch size, and regularization terms can likewise be tuned more systematically.

Another interesting direction is to understand why the LiteMono + PCV model achieves a lightweight model in terms of parameters, yet does not yield a proportionally large reduction in inference time.

Finally, the trained models can be further evaluated on other benchmark datasets to examine their generalization ability and robustness across different domains and acquisition conditions.

5. Conclusion

In this work, I systematically explore three lightweight variants of SupDepth4Thermal for both monocular and stereo depth estimation. For MDE, replacing the original backbone with LiteMono significantly reduces model complex-

352

353

354

355

356

357

358

359

360

361

362

363

364

365

366

367

368 ity, but the error metrics in Tab. 3 show a clear degradation
 369 compared to the SupDepth4Thermal monocular baseline,
 370 indicating that the current integration is not yet competitive
 371 in terms of accuracy.

372 For SDE, the depthwise separable decoder and the Lite-
 373 Mono encoder plus PCV strategy both succeed in making
 374 the stereo network substantially more lightweight in terms
 375 of parameter count and FLOPs, as summarized in Tab. 5.
 376 However, this comes with an increase in disparity error
 377 across different settings, meaning that efficiency gains are
 378 achieved at the cost of prediction quality.

379 Overall, these results highlight a classic accuracy–efficiency trade-off. The overly simplified architecture leads to nontrivial increases in error. To close this gap, exploring alternative encoder-decoder designs and improving the cost volume computation algorithm are vital directions for future work.

385 References

- [1] Hu Cao, Yueye Wang, Joy Chen, Dongsheng Jiang, Xiaopeng Zhang, Qi Tian, and Manning Wang. Swin-unet: Unet-like pure transformer for medical image segmentation. In *European conference on computer vision*, pages 205–218. Springer, 2022. 2
- [2] Yukyung Choi, Namil Kim, Soonmin Hwang, Kibaek Park, Jae Shin Yoon, Kyounghwan An, and In So Kweon. Kaist multi-spectral day/night data set for autonomous and assisted driving. *IEEE Transactions on Intelligent Transportation Systems*, 19(3):934–948, 2018. 3
- [3] François Fleuret. Xception: Deep learning with depthwise separable convolutions. In *Proceedings of the IEEE conference on computer vision and pattern recognition*, pages 1251–1258, 2017. 3
- [4] Weichen Dai, Yu Zhang, Shenzhou Chen, Donglei Sun, and Da Kong. A multi-spectral dataset for evaluating motion estimation systems. In *2021 IEEE International Conference on Robotics and Automation (ICRA)*, pages 5560–5566. IEEE, 2021. 3
- [5] Devansh Dhrafani, Yifei Liu, Andrew Jong, Ukcheol Shin, Yao He, Tyler Harp, Yaoyu Hu, Jean Oh, and Sebastian Scherer. Firestereo: Forest infrared stereo dataset for uas depth perception in visually degraded environments. *IEEE Robotics and Automation Letters*, 2025. 3
- [6] Andreas Geiger, Philip Lenz, Christoph Stiller, and Raquel Urtasun. Vision meets robotics: The kitti dataset. *The international journal of robotics research*, 32(11):1231–1237, 2013. 3, 4
- [7] Andrew G Howard, Menglong Zhu, Bo Chen, Dmitry Kalenichenko, Weijun Wang, Tobias Weyand, Marco Andreetto, and Hartwig Adam. Mobilenets: Efficient convolutional neural networks for mobile vision applications. *arXiv preprint arXiv:1704.04861*, 2017. 3
- [8] Alex Junho Lee, Younggun Cho, Young-sik Shin, Ayoung Kim, and Hyun Myung. Vivid++: Vision for visibility dataset. *IEEE Robotics and Automation Letters*, 7(3):6282–6289, 2022. 3
- [9] Peize Li, Kaiwen Cai, Muhamad Risqi U Saputra, Zhuangzhuang Dai, and Chris Xiaoxuan Lu. Odombeyondvision: An indoor multi-modal multi-platform odometry dataset beyond the visible spectrum. In *2022 IEEE/RSJ International Conference on Intelligent Robots and Systems (IROS)*, pages 3845–3850. IEEE, 2022. 3
- [10] Lahav Lipson, Zachary Teed, and Jia Deng. Raft-stereo: Multilevel recurrent field transforms for stereo matching. In *2021 International Conference on 3D Vision (3DV)*, pages 218–227. IEEE, 2021. 4
- [11] Ze Liu, Yutong Lin, Yue Cao, Han Hu, Yixuan Wei, Zheng Zhang, Stephen Lin, and Baining Guo. Swin transformer: Hierarchical vision transformer using shifted windows. In *Proceedings of the IEEE/CVF international conference on computer vision*, pages 10012–10022, 2021. 2
- [12] Yawen Lu and Guoyu Lu. An alternative of lidar in nighttime: Unsupervised depth estimation based on single thermal image. In *Proceedings of the IEEE/CVF Winter Conference on Applications of Computer Vision*, pages 3833–3843, 2021. 1
- [13] Nikolaus Mayer, Eddy Ilg, Philip Hausser, Philipp Fischer, Daniel Cremers, Alexey Dosovitskiy, and Thomas Brox. A large dataset to train convolutional networks for disparity, optical flow, and scene flow estimation. In *Proceedings of the IEEE conference on computer vision and pattern recognition*, pages 4040–4048, 2016. 4
- [14] Pierluigi Zama Ramirez, Fabio Tosi, Matteo Poggi, Samuele Salti, Stefano Mattoccia, and Luigi Di Stefano. Open challenges in deep stereo: the booster dataset. In *Proceedings of the IEEE/CVF Conference on Computer Vision and Pattern Recognition*, pages 21168–21178, 2022. 4
- [15] Leonardo Ravaglia, Roberto Longo, Kaili Wang, David Van Hamme, Julie Moeyersoms, Ben Stoffelen, and Tom De Schepper. Rgb-to-infrared translation using ensemble learning applied to driving scenarios. *Journal of Imaging*, 11(7):206, 2025. 2
- [16] Daniel Scharstein, Heiko Hirschmüller, York Kitajima, Greg Krathwohl, Nera Nešić, Xi Wang, and Porter Westling. High-resolution stereo datasets with subpixel-accurate ground truth. In *German conference on pattern recognition*, pages 31–42. Springer, 2014. 4
- [17] Ukcheol Shin, Jinsun Park, and In So Kweon. Deep depth estimation from thermal image. In *Proceedings of the IEEE/CVF Conference on Computer Vision and Pattern Recognition*, pages 1043–1053, 2023. 1, 3
- [18] Yihong Sun and Bharath Hariharan. Dynamo-depth: Fixing unsupervised depth estimation for dynamical scenes. *Advances in Neural Information Processing Systems*, 36: 54987–55005, 2023. 2
- [19] Wayne Treibert, Philip Saponaro, Scott Sorensen, Abhishek Kolagunda, Michael O’Neal, Brian Phelan, Kelly Sherbondy, and Chandra Kambhamettu. Cats: A color and thermal stereo benchmark. In *Proceedings of the IEEE Conference on Computer Vision and Pattern Recognition*, pages 2961–2969, 2017. 3
- [20] Diana Wofk, Fangchang Ma, Tien-Ju Yang, Sertac Karaman, and Vivienne Sze. Fastdepth: Fast monocular depth esti-

- 480 mation on embedded systems. In *2019 International Conference on Robotics and Automation (ICRA)*, pages 6101–6108.
481 IEEE, 2019. 1, 3
- 482 [21] Weihao Yuan, Xiaodong Gu, Zuozhuo Dai, Siyu Zhu, and
483 Ping Tan. Neural window fully-connected crfs for monocular depth estimation. In *Proceedings of the IEEE/CVF conference on computer vision and pattern recognition*, pages 3916–3925, 2022. 2
- 484 [22] Jiaxi Zeng, Chengtang Yao, Lidong Yu, Yuwei Wu, and
485 Yunde Jia. Parameterized cost volume for stereo matching.
486 In *Proceedings of the IEEE/CVF International Conference on Computer Vision*, pages 18347–18357, 2023. 1
- 487 [23] Ning Zhang, Francesco Nex, George Vosselman, and Norman Kerle. Lite-mono: A lightweight cnn and transformer
488 architecture for self-supervised monocular depth estimation.
489 In *Proceedings of the IEEE/CVF conference on computer vision and pattern recognition*, pages 18537–18546, 2023. 1
- 490 [24] Hengshuang Zhao, Jianping Shi, Xiaojuan Qi, Xiaogang
491 Wang, and Jiaya Jia. Pyramid scene parsing network. In *Proceedings of the IEEE conference on computer vision and
492 pattern recognition*, pages 2881–2890, 2017. 2
- 493 [25] Xingxing Zuo, Nikhil Ranganathan, Connor Lee, Georgia
494 Gkioxari, and Soon-Jo Chung. Monother-depth: Enhancing
495 thermal depth estimation via confidence-aware distillation.
496 *IEEE Robotics and Automation Letters*, 2025. 2
- 497
- 498
- 499
- 500
- 501
- 502
- 503
- 504